Thermokinetic Actuation for Batch Assembly of Microscale Hinged Structures

Ville Kaajakari and Amit Lal

***Abstract*—This paper reports on surface micromachined hinged structure assembly using thermokinetic forces in the molecular flow regime. Ultrasonic vibration energy is used to reduce the static friction making the thermokinetic force comparatively significant. The thermokinetic force, resulting from the more energetic gas molecules emanating from the heated substrate, increases with pressure and substrate temperature in the molecular flow regime. The transition from viscous to molecular regime occurs as the molecular mean-free-path approximately equals the flap length, making the pressure threshold for thermokinetic flap actuation size dependent. In addition to the experimental results, one-dimensional (1-D) and two-dimensional (2-D) force models are presented. Examples of assembled structures are shown and assembly jig suitable for automated MEMS batch assembly is demonstrated. [847]**

***Index Terms*—Batch assembly, microelectromechanical systems (MEMS), thermal actuation.**

I. Introduction

HINGED structures enable three-dimensional (3-D) components with surface micromachining techniques and have found applications for example in optical and RF systems. In the past, different assembly methods have been proposed for surface micromachined flaps. The structures can be assembled manually using a probe tip, but due to the labor and time cost of manual assembly, automated solutions are being investigated. One way is to use on-chip electrostatic [1] or thermal actuators [2]. This is attractive especially if the resulting devices need to be actuated during the device operation. A major drawback is the large die surface area consumed by the actuators. Other methods have been proposed that use special processing or external actuation forces. Thermal shrinkage of polyimide in V-grooves [3] and surface tension of wet solder [4] have been used to lift and permanently assemble micromachined flaps into the upright position. External magnetic forces can be used to actuate surface micromachines either by passing current through them (Lorentz force) [5] or by depositing magnetic material on them [6].

Here we report on the use of gas kinetics to actuate and assemble hinged microstructures. The thermal actuation is due to differential force on the flap near heated surface in the molecular flow regime. As illustrated in Fig. 1, the higher energy particles emitted from the hotter surface lead to net force lifting the flaps. This phenomenon is similar to the well described "radiometer effect" [7]. As only heat and vacuum are required, the method is suitable for actuating devices from *any* surface micromachining process. Furthermore, no surface area is consumed nor are any interconnects required on the silicon die. The history of radiometer effect dates back to the original Crooke's radiometer (1873), a four-vaned device with dark and light surfaces, that rotates when a source of light is brought nearby. The radiometer mechanism was explained by Knudsen (1910) with energy transfer from heated dark surface to gas molecules generating recoil force. Knudsen also proposed an absolute manometer based on the momentum transfer between two heated surfaces although the device has not been commercially adopted due to its delicate nature.

The thermokinetic force described here is usually smaller than the frictional forces encountered in moving polysilicon microstructures. However, in this work ultrasonic vibrations are used to reduce the friction to make the thermokinetic force comparatively significant. The silicon sample was ultrasonically vibrated using an adhesively or suction bonded piezoelectric PZT (lead-zirconate-titanate oxide) plate. Ultrasonic vibrations have previously been used for assembly as a source of random energy input [8]. In the work presented here, however, the purpose of the vibrations was only to remove friction and not to move the microstructures. The sample was vibrated at high frequencies ($>$2.5 MHz), where the vibration amplitude is only a few nanometers and is not sufficient to impact actuate the surface micromachines.

This paper is organized as follows: 1) Relevant forces on surface micromachined hinged structures are analyzed as a function of ambient pressure and temperature. 2) Experimental set-up and results of using gas kinetics to assemble surface micromachines are presented. 3) The paper is then concluded with examples of assembled surface micromachined structures.

II. Analysis of Forces on a Hinged Structure

In this section the role of gravity, friction, ultrasonic vibrations, and gas-kinetic forces are compared in the context of surface micromachined flaps and relevant pressure regimes are identified.

A. Gravity Force and Hinge Friction

Gravity and other inertial forces are the dominant forces in macro scale structures. However, as the mechanical devices shrink to micron scale, surface forces dominate. For a silicon plate with dimensions of 100 μm $\times$ 250 μm $\times$ 2 μm, the gravity force ($F_{\mathrm{grav}} = mg$) is only 0.4 nN, while friction

Manuscript received April 7, 2002; revised September 24, 2002. This work was supported by an NSF-CAREER award. Subject Editor G. K. Fedder.

V. Kaajakari is with VTT Information Technology, FIN-02044, Finland.

A. Lal is with the School of Electrical and Computer Engneering, Cornell University, Ithaca, NY 14853 USA (e-mail: lal@ece.cornell.edu).

Digital Object Identifier 10.1109/JMEMS.2003.811747

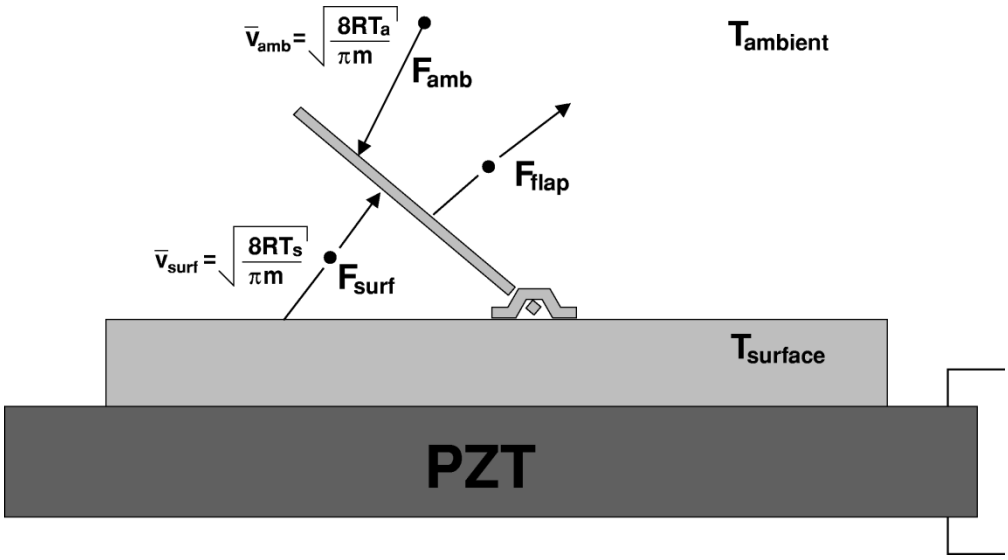

Fig. 1. The origin of thermokinetic force. Gas molecules impacting the flap from the heated surface have higher momentum than those from the ambient gas. Forces due to molecules leaving both sides of the flap cancel. Ultrasonic vibrations are used to reduce hinge friction.

force can be an order of magnitude larger. To remove the hinge friction, the substrate was vibrated at ultrasonic frequencies with continuous sweep from 2.5 MHz to 6 MHz. The swept frequency actuation ensures the excitation of several bulk modes of the PZT/Si composite. The vibrations cause the hinge-flap contact to break and the friction force vanishes momentarily as observed in ultrasonic AFM [9] and destiction experiments [10]. This stick-slip contact at MHz frequencies results in overall reduction of frictional force. While the process is under further investigation, the friction reduction theory is strongly supported by the fact that the observed flap movement due to thermokinetic actuation is significantly reduced without ultrasound.

B. Impact From Sonic Pulses

Substrate vibrations can be used to actuate surface micromachines [11], [12]. This can be accomplished by exciting the substrate at the surface micromachine resonance for frequency selective actuation, or by pulsing the entire substrate for impact actuation. In the work presented here, however, the purpose of the substrate vibrations was to remove static friction and not to cause actuation. Therefore the vibration amplitude was kept below the impact actuation threshold.

C. Thermokinetic Forces

In this section, a first order one-dimensional (1-D) model for thermokinetic force is developed. It is assumed that the intermolecular collisions are not significant, which confines the model to low pressure regime, where the mean free path is much greater that the device dimensions. However, the effect of intermolecular collisions is analyzed qualitatively and three different pressure regimes for the dominant force are obtained. Furthermore, it is assumed that the molecular flux is constant throughout the vacuum chamber. This assumption is valid in the absence of intermolecular collisions even with different surface temperatures. Finally, it is assumed that the ambient wall temperature is constant and not affected by the heated sample surface.

The origin of thermokinetic force is illustrated in Fig. 1. The gas molecules from ambient gas with temperature T_{ambient} bombard the die surface and flaps with average velocity $\overline{v}_{\text{ambient}} = \sqrt{8RT_{\text{ambient}}/\pi m}$ [13]. These molecules are absorbed and accommodated on the surfaces. After a finite amount of time they desorb leaving the surface with average velocity $\overline{v}_{\text{surface}}$ corresponding to the effective surface temperature $T^{\text{eff}}_{\text{surface}}$. If the surface temperature is higher than the ambient, molecules leaving the surface impact the flap with higher average momentum than the ambient molecules. The forces due to molecules leaving both sides of the flap cancel as the two surfaces are at the same temperature and are impinged by the same molecular flux. The constant temperature assumption follows from the flap being thin (2 μm) and made of polysilicon, which is a good thermal conductor.

The effective temperature $T^{\text{eff}}_{\text{surface}}$ of desorbing molecules depends on how long the gas molecules stay absorbed on the surface and can be expressed as

$$T^{\text{eff}}_{\text{surface}} = \alpha(T_{\text{surface}} - T_{\text{ambient}}) + T_{\text{ambient}} \tag{1}$$

in terms of the phenomenological accommodation coefficient α $(0 < \alpha < 1)$ and the ambient and surface temperatures T_{ambient} and T_{surface}. The case of $\alpha = 0$ corresponds to elastic surface-molecule interaction with no change in molecule temperature. The case of $\alpha = 1$ correspond to full accommodation $(T^{\text{eff}}_{\text{surface}} = T_{\text{surface}})$. Typically $\alpha > 0.8$ for collision between engineering surfaces and heavy molecules such as N_2 [14].

The force from the impacting (absorbing) molecules on a surface area A is given by

$$F_{\text{absorb}} = \frac{1}{2}AP = \frac{1}{2}A\frac{\pi m\overline{v}\Phi}{2} \tag{2}$$

where P is gas pressure, m is mass, and Φ is the molecular incidence rate or molecular flux. The half factor is due to pressure being exerted on the surface in two steps: impact from absorption and desorption. The molecular incidence rate is given by

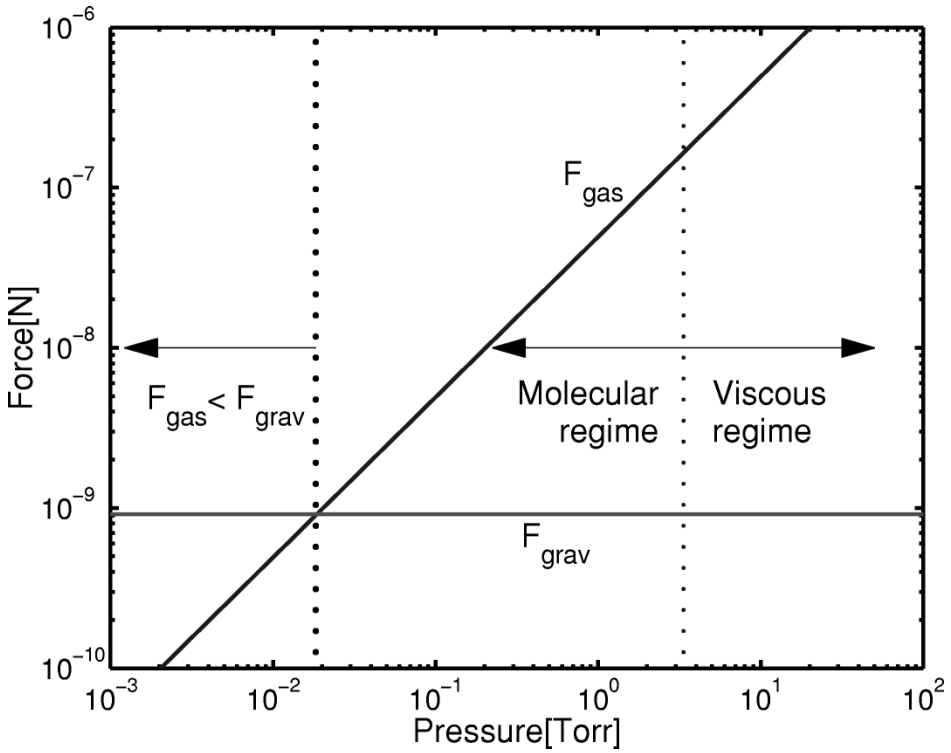

Fig. 2. Thermokinetic force and gravity force with $T^{eff}_{surface} = 100°$C. Above ~10 torr (viscous regime), there is no net force on the flaps. Below ~10 torr (molecular regime), the flaps feel net force upwards. The gravity force dominates below ~10 mtorr. The graph is for a polysilicon plate with dimensions of $200\ \mu$m $\times$ $100\ \mu$m $\times$ $2\ \mu$m.

$\Phi = (1/4)n\overline{v} = (P/\sqrt{2\pi mkT_{\text{ambient}}})$, where n is the number of molecules per unit volume. The total force on the flap can be calculated by taking the difference of the force from the absorbing molecules from the ambient-facing and substrate-facing sides leads. Thus we have

$$F_{\text{flap}} = \frac{1}{2}AP\left(\frac{\overline{v}_{\text{surface}}}{\overline{v}_{\text{ambient}}} - 1\right) = \frac{1}{2}AP\left(\sqrt{\frac{T^{\text{eff}}_{\text{surface}}}{T_{\text{ambient}}}} - 1\right). \tag{3}$$

For the flaps to lift up, there must be a small initial gap between the flap and the substrate surface. Here this is accomplished with dimples on the flap that keep it above the surface. The dimples also reduce the flap-surface contact area and thus reduce the adhesive forces that could cause the flap to stay stuck on the surface. Etch holes on the flap also serve as entry points for molecules to initiate actuation of a plate initially lying flat on the surface. For flap dimensions of $100\ \mu$m $\times$ $250\ \mu$m, pressure of 500 mtorr, accommodation coefficient $\alpha = 1$, and surface and ambient temperatures of 100 °C and 20 °C, respectively, (3) gives $F_{\text{gas}} = 85$ nN. Although this force is small, it is still two orders of magnitude greater than the gravity force for silicon flaps with same area and thickness of 2 μm.

Since the gas force depends on pressure, different regimes of operation are observed as illustrated in Fig. 2. In the viscous regime, the gas molecules leaving the substrate equilibrate with ambient before impacting the flap and there is no net force. As the pressure is decreased, the mean-free path ($\lambda = 5 \cdot 10^{-3} P^{-1}$ cm $\cdot$ torr in air) increases and becomes comparable to the flap dimensions [15]. The molecules impacting the flap result in a net force perpendicular to the substrate. Thus, the flaps are lifted up at pressure corresponding to transition pressure from viscous to molecular flow at the flap scale (at $P = 1$ torr, $\lambda \approx 50\ \mu$m). Short flaps are expected to lift up at a higher pressure than tall flaps. The flaps stabilize perpendicular to substrate, as momentum from impacting molecules is equal on both sides of the flaps. Below the transition pressure, the force diminishes linearly with decreasing pressure in accordance with (3) as the particle density is reduced. Eventually the thermokinetic force becomes less than other forces such as gravity and ultrasonic forces.

III. 2-D Force Model in Low-Pressure Regime

To calculate the thermokinetic force as a function of flap angle, the 1-D model presented in the previous section is expanded to take the geometry effects into account as shown in Fig. 3. For simplicity the flap and the substrate are assumed to be infinite in y-direction. The net moment on the flap with respect to the hinge is calculated by summing the moments from the ambient gas molecules, the surface desorbed molecules, and the moment due to gravity. The moment due to molecules desorbed from the bottom and topside of the flap cancel as these surfaces are at the same temperature. It is assumed that the flap and the substrate size are small compared to the mean free path of the gas molecules, a condition easily obtained experimentally. In this pressure regime, the gas molecules do not interact with each other.

The number of molecules striking the surface per unit area from a solid angle Ω is given by

$$\mathrm{d}\Phi = \frac{n\overline{v}_{\text{ambient}}}{4}\frac{\cos(\theta)}{\pi}\mathrm{d}\Omega \tag{4}$$

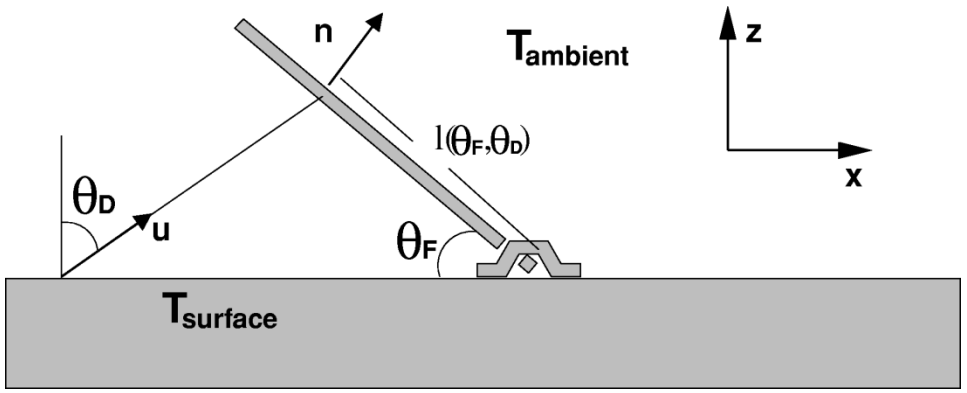

Fig. 3. Two-dimensional model to account for flap geometry and angle.

where θ is the angle of impinging molecules with respect to the surface normal. The mean magnitude of momentum for ambient gas molecules is

$$p = \frac{3}{2}\sqrt{\frac{\pi m k T_{\text{ambient}}}{2}}. \tag{5}$$

Thus the total downward force due to ambient gas on the top side is obtained by integrating the product of molecular flux and mean momentum perpendicular to the surface over all the possible directions. This can be expressed as

$$F_{\text{down}}^{\text{amb}} = \int_{\Omega} \cos(\theta) p \, \mathrm{d}\Phi = \frac{3}{8}\pi m \bar{v}_{\text{ambient}} \Phi \int_{\frac{\pi}{2}-\theta_F}^{\frac{\pi}{2}} \cos^2(\theta)\sin|\theta| \mathrm{d}\theta \int_{\frac{-\pi}{2}}^{\frac{\pi}{2}} \mathrm{d}\varphi. \tag{6}$$

Carrying out the integration for the downward force per unit area results in

$$F_{\text{down}}^{\text{amb}} = \frac{1}{8}\pi m \bar{v}_{\text{ambient}} \Phi \left(1 + \cos^3(\theta_F)\right) \mathrm{d}A. \tag{7}$$

The downward moment per unit length in y-direction is obtained by integrating the force times lever arm length over the flap length resulting in

$$M_{\text{push}}^{\text{amb}} = \frac{1}{8} P L^2 \left(2 - \sin^3(\theta_F)\right). \tag{8}$$

Similarly, the lift moment from underside side of the flap due to ambient gas is given by

$$M_{\text{lift}}^{\text{amb}} = \frac{1}{8} P L^2 sin^3(\theta_F). \tag{9}$$

For moments due to molecules desorbed from the die surface, no simple closed form solution can be derived. The moment is obtained by numerically integrating the contributions over the entire substrate. The number of molecules desorbed from unit area to the direction $\mathbf{u}$ is given by

$$N_D = \Phi \frac{\cos(\theta_D)}{\pi} \tag{10}$$

where θ_D is the angle between the surface normal and $\mathbf{u}$. The mean momentum of desorbed molecules is

$$p = \frac{3}{2}\sqrt{\frac{\pi m k T_{\text{surface}}^{\text{eff}}}{2}}. \tag{11}$$

The moment due to a substrate unit area $\mathrm{d}A$ is obtained by integrating the product of p and N_D (the mean momentum and number of desorbed molecules) over the possible solid angles

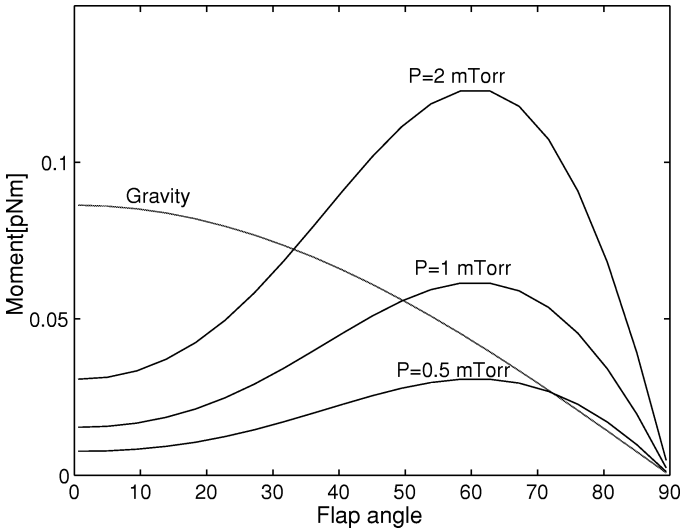

Fig. 4. Calculated gas-kinetic and gravity moments from 2-D model ($\alpha = 1$, $T_{\text{surface}}^{\text{eff}} = 100\ ^{\circ}\text{C}$).

formed toward the flap. This differential momentum can be written as

$$dM_{\text{surface}} = \int_{\Omega} \frac{3}{4\pi} P \sqrt{\frac{T_{\text{surface}}^{\text{eff}}}{T_{\text{ambient}}}} \mathbf{u}\cdot\mathbf{n} \cos(\theta_D) l(\theta_D, \theta_F) \mathrm{d}\Omega. \tag{12}$$

Here $l(\theta_D, \theta_F)$ is the moment arm of the impinging molecules, and $\mathbf{u}\cdot\mathbf{n}$ is due to fact that only the velocity component perpendicular to the flap surface contributes to the moment. The total moment M_{surface} is obtained by integrating (12) over the entire substrate. On the other hand, the moment due to gravity is given by

$$M_{\text{gravity}} = \frac{1}{2} m g \cos(\theta_F) L. \tag{13}$$

Fig. 4 shows the magnitude of gas-kinetic and gravity moments calculated from the 2-D model at $T_{\text{surface}}^{\text{eff}} = 100\ ^{\circ}\text{C}$. For a flap lying on the surface ($\theta_F = 0$), the 1-D and 2-D models give the same moment. However, the gas-kinetic moment is shown to increase as the flap is lifted up and has a maximum at angle of 60°. As the angle is increased further, the force decreases. For a fully erected flap, all the moments cancel and the flap is at a stable point. The maximum moment from the 2-D model is about 4 times more than the moment obtained by integrating

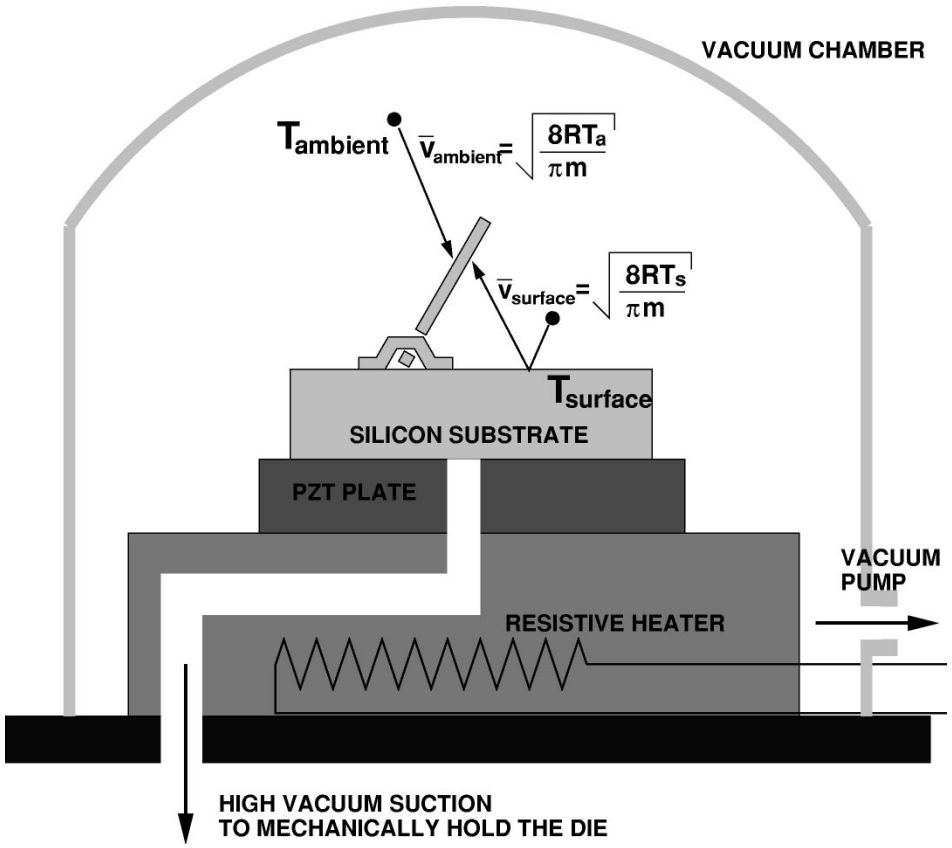

Fig. 5. Experimental apparatus. The two vacuum ports are for maintaining differential pressure over the die for suction attachment.

the 1-D force (3). As the pressure is lowered, the moment due to gravity overcomes the gas-kinetic moment barrier, and the flaps fall down.

IV. Experimental Apparatus and Procedures

For the experiments a temperature controlled PZT assembly mount shown in Fig. 5 was fabricated. The PZT plate with dimensions of 10 mm $\times$ 10 mm $\times$ 0.2 mm was soldered to a hot plate with temperature control to adjust the substrate temperature. This assembly mount was placed in a vacuum chamber and the chamber pressure was adjusted in the range of 1 mtorr to 750 torr with a leak valve. The sample was monitored with an optical microscope, and the video image together with substrate temperature and chamber pressure were electronically recorded. Charge effects were minimized by sputtering 200 Å of gold on both sides of the released flaps by flipping the flaps over in between two sputter coatings. Eliminating the electrostatic effects is especially important as initial studies indicated that surface charging could be a possible actuation mechanism [16].

In experiments requiring vacuum pressures less than 500 mtorr, the silicon die was mounted to the PZT with adhesive bonding. This can be undesirable in an industrial environment. Therefore vacuum suction for holding down the silicon die was investigated. It was found that even in moderate vacuum ($>$0.5 torr), suction is enough to hold the die in place during the assembly. At lower chamber pressures, the pressure difference between the suction pipe and chamber was too low to hold the die during ultrasonic vibrations. An alternative to the suction would be to use mechanical clamping, which is under investigation. The fact that imperfect mechanical coupling of ultrasonic vibrations without adhesive also leads to assembly indicates that the ultrasound serves only to reduce friction. This vacuum jig allows quick attachment of the die to the assembly tool enabling *automated* assembly of MEMS.

The PZT/silicon substrate resonance frequencies depend on device geometry and material properties and change with temperature. To avoid complications of frequency, the actuation frequency was swept from 2.5 to 5 MHz with excitation amplitude of approximately 10 V_{PP}. The swept frequency actuation also has the advantage over fixed frequency actuation that there are no fixed nodal patterns and micromachines are excited more evenly over the entire surface leading to more uniform friction reduction across the die. The high frequency range was chosen because frequencies less than 1 MHz can excite strong lateral and bending vibrations of the substrate. These sub 1 MHz vibrations can have large vibration amplitude ($\sim 1-2\mu$m) at the anti-nodes, sufficient to impact actuate or even break the surface micromachines.

V. Experimental Results

In the first set of experiments, the flap actuation was observed as the chamber pressure was lowered. The substrate temperature was set to 100 °C and ultrasound was applied to reduce friction. In the viscous regime (10–750 torr) the flaps stay down as expected as the mean free path is too small to generate significant actuation force. As the pressure is lowered to below 10 torr first

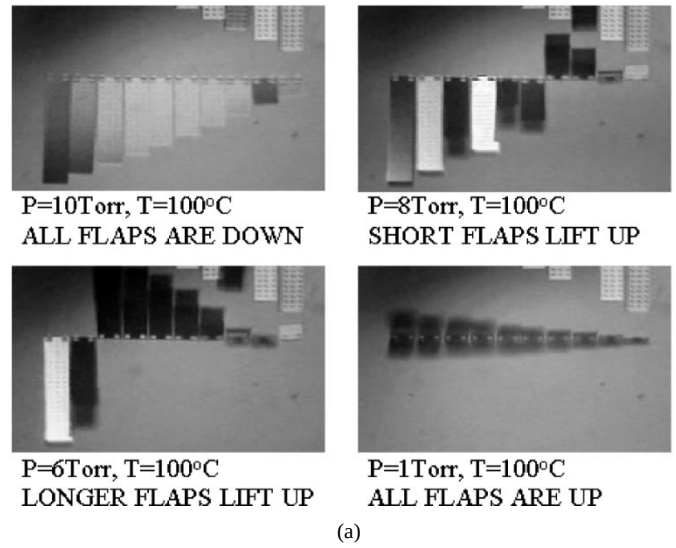

(a)

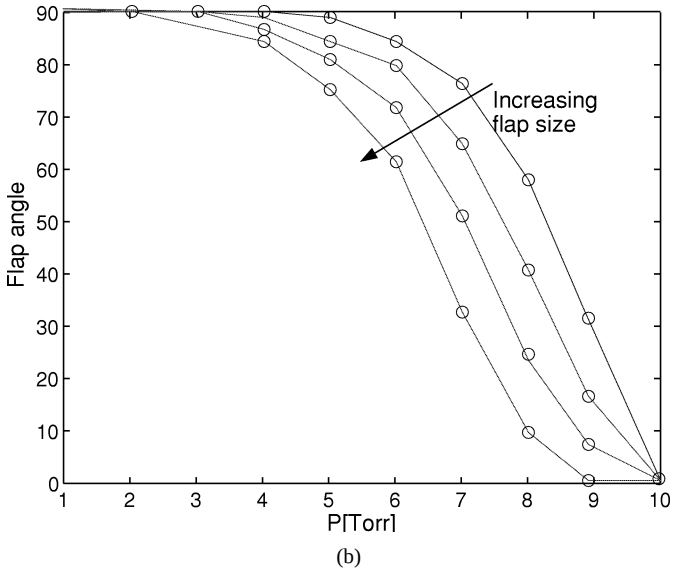

(b)

Fig. 6. The effect of flap length on the transition pressure from viscous to molecular flow. As the chamber pressure is lowered, shorter flaps are lifted before longer ones. The angle versus pressure data is for flap lengths of 200, 300, 400, and 500 μm.

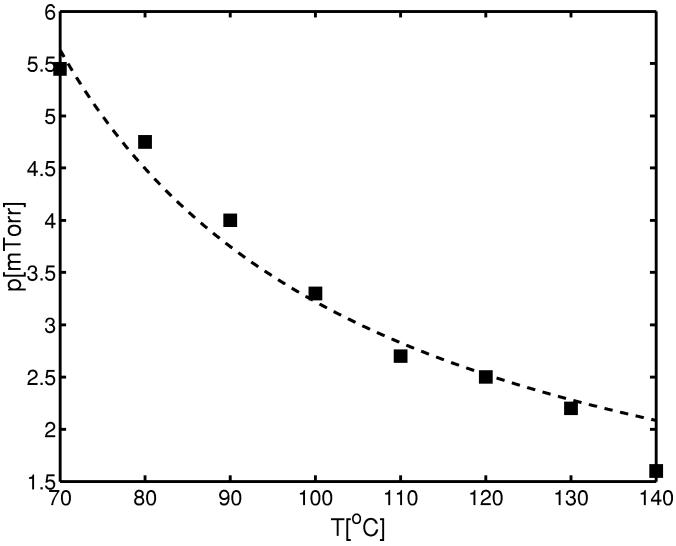

Fig. 7. Measured flap falling pressure thresholds versus substrate temperature and the theoretical p-T curve (flap lengths 100–500 μm).

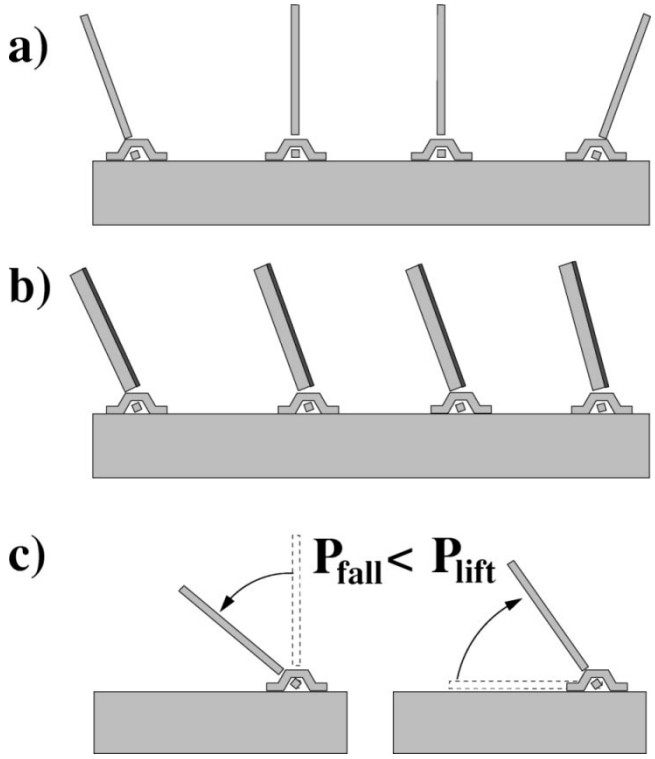

Fig. 8. Observed 3-D effects. (a) Flaps at the edge of the die stand in a slight angle. These flaps will also fall before the middle flaps as the pressure is lowered to gravity dominant regime. (b) Heavy flaps with gold coating would not lift fully at low $T_{\rm surface}$ but have a stable point around the moment maximum. (c) The transition pressure from thermokinetic to gravity dominant regime depends on the flap angle.

short flaps and then longer flaps lift up, confirming that the transition pressure depends on the flap dimensions (Fig. 6). After ultrasound removal and cooling of the sample, the assembled flaps remain in the vertical position indefinitely due to static friction at the hinges. Applying ultrasound to the samples after removing the thermokinetic force by cooling the sample resulted in flaps falling down. It should be noted that some of the flaps would lift up when heated at lowered pressure even without the ultrasonic friction removal due to statistical nature of the hinge friction. This also demonstrates that ultrasound is not the source of actuation.

In the next experiment, the low pressure behavior of the thermokinetic force on the flaps was verified. As pressure is lowered the thermokinetic force becomes smaller than the gravity force. The fact that the flaps fall down due to gravity and not other, for example ultrasound induced forces, was verified by mounting the sample at different angles. As the pressure is lowered, the flaps fall down toward the declining tilt. Unfortunately, the 1-D and 2-D models give different transition pressure with 1-D model overestimating and 2-D model underestimating the fall down pressure. Possible explanations for the 2-D model overestimating the force are that the accommodation coefficient being less than unity and the heating of the ambient gas. Both these effects would lower the thermokinetic force. A good agreement, however, is obtained

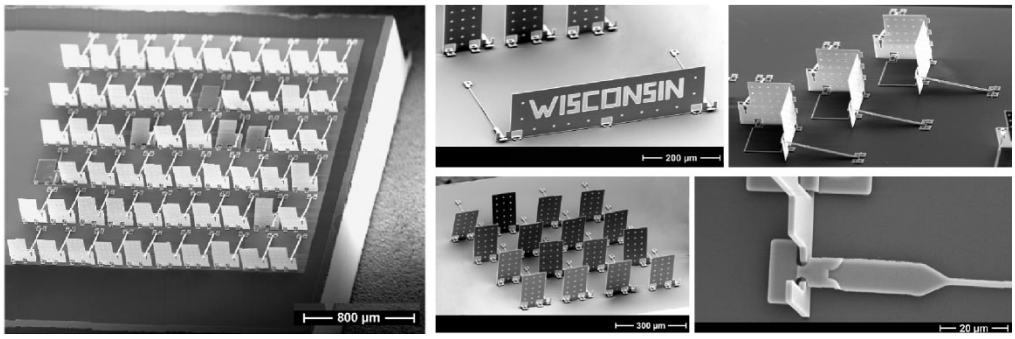

Fig. 9. Examples of assembled devices. Left: 10×6 parallel assembled array (some flaps fell down after assembly due to lack of spring latch). Top right: "Micro-art" Wisconsin banner and polysilicon corner cube reflectors (200×200 μm) with lock-in structure. Bottom right: Array of assembled micromachined flaps with spring latch, and close-up of the latch.

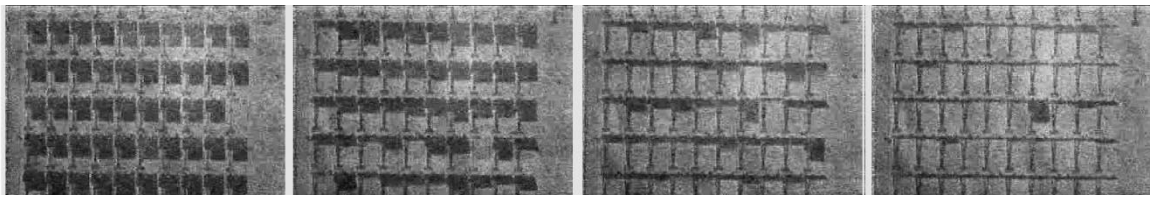

Fig. 10. Snapshots of a flap array assembly (50×200 μm flaps, 10×6 array). 1. Flaps are vibrating on the surface. 2–4. Flaps are lifting up. 5. All but one flap are lifted (SEM photo identified the problem to be a dirt particle).

with the 1-D model by introducing an empirical correction factor C to the gas-kinetic force and rewriting (3) as

$$F_{\text{gas}} = \frac{1}{2} CAp \left(\sqrt{\frac{T_{\text{surface}}^{\text{eff}}}{T_{\text{ambient}}}} - 1 \right). \tag{14}$$

Similar geometry dependent correction factors have been used previously in modeling Knudsen radiometer gauges [17]. At the transition pressure $F_{\text{gas}} = F_{\text{gravity}}$ and since $F_{\text{gravity}} = mg = \rho Ahg$, where g is the gravity constant and m, ρ, A, h are the flap mass, density, area and thickness respectively, the fall down transition pressure can be written as

$$P_{\text{transition}} = \frac{2\rho hg}{C\left(\sqrt{\frac{T_{\text{particle}}}{T_{\text{ambient}}}} - 1 \right)} \tag{15}$$

which is independent of the flap area. Fig. 7 shows the measured data in good agreement with theoretical curve with $C = 2$. Also, flaps with areas varying an order of magnitude all fall down at the same pressure confirming the area independence of the fall down pressure.

VI. Observed 3-D Effects

In addition to pressure threshold experiments described in the previous section, several effects due to 3-D nature of gas-kinetic actuation were observed as shown in Fig. 8. Flaps at the edge of the die have a stable point in a slight outward angle due to higher number of desorbed molecules from the center of the die. The flaps at the edges would also fall down at a slightly higher pressure than the flaps at the center due to different net moments. Also, at moderate surface temperatures (~ 60 °C) heavy flaps (3.5 μm thick with 0.5 μm gold film) would not fully lift up but would stand at an approximate angle of $45 \pm 5°$ in agreement with the predicted force maximum at that angle (Fig. 4). Finally, the transition pressure at which the thermokinetic force is greater than the gravity force depends on the flap angle. The flaps would fall down at a lower pressure than they would lift up, as the pressure was increased and decreased around the transition point. This hysteresis follows from the angle dependence of the thermokinetic force. These observations qualitatively confirm the 2-D gas-kinetic model.

VII. Assembly of Flap Structures

For permanent assembly one requires the assembled structures to stay in their final position even after the gas-kinetic force is removed. Therefore structures with locking mechanisms were also fabricated in MUMP's process. Such locking structures have been used extensively in manual assembly procedure [18]. Fig. 9 shows examples of assembled flap arrays and retroreflectors. One observed problem with early experiments was that the hinged locking latch failed to lock down properly due to thermokinetic upwards force acting on it. This caused some flaps to fall down after assembly as shown on the left side of Fig. 9. This problem can be solved by using a spring latch anchored to the substrate thus providing the downwards latching force as shown in the examples of assembled arrays on the right side of Fig. 9. Fig. 10 shows video images of the array assembly at different times. Nearly 100% assembly yields are obtained in 30 s. The failures are due to incomplete release, stiction or mechanical jamming at the hinge or the latch.

VIII. Discussion

A novel batch assembly mechanism for surface micromachines is demonstrated. The forces on the surface structures are characterized as a function of pressure and temperature and three pressure regimes are identified. In the viscous regime, the drag forces dominate. In the molecular flow regime, the thermokinetic forces are significant but decrease with pressure

due to reduced particle density. At pressures less than 10 mtorr, the thermokinetic force becomes negligible. The thermokinetic force is limited by the pressure and temperature. Since the maximum operating pressure is limited by the requirement of mean free path being larger than the critical dimensions, the force can only be increased by increasing the surface-ambient temperature difference. Assuming maximum surface temperature of $500\ ^{\circ}\mathrm{C}$, ambient temperature of $25\ ^{\circ}\mathrm{C}$ and pressure of 1 torr gives force of $40\ \mu\mathrm{N/mm}^2$. In designing lock-in structures for assembly, the force limitation should be taken into account.

A PZT vibrator/heater jig that does not require adhesive bonding to the silicon is also demonstrated enabling bath assembly in an industrial setting. Such a tool will allow surface micromachine designers to design complicated structures that can be assembled within minutes without the need for any special processing, interconnect requirements, or real-estate overhead. In addition, the thermokinetic actuation scheme provides a thermodynamic actuation methodology for surface micromachines.

ACKNOWLEDGMENT

The authors would like to acknowledge Wisconsin Center for Applied Microelectronics (WCAM) for technical support in device processing.

REFERENCES

[1] N. C. Tien, O. Solgaard, M.-H. Kiang, M. Daneman, K. Y. Lau, and R. S. Muller, "Surface-micromachined mirrors for laser-beam positioning," *Sensors and Actuators A*, vol. A52, no. 1–3, pp. 76–80, Mar. 1996.

[2] J. R. Reid, V. M. Brigth, and J. T. Butler, "Automated assembly of flip-up micromirrors," *Sens. Actuators, Phys. A*, vol. 66, no. 1–3, pp. 292–298, Apr. 1998.

[3] T. Ebefors, E. Kälvesten, and G. Stemme, "New small radius joints based on thermal shrinkage of polyimide in V-grooves for robust self-assembly 3D microstructures," *J. Micromech. Microeng.*, vol. 8, no. 3, pp. 188–194, Sep. 1998.

[4] R. A. A. Syms, "Equilibrium of hinged and hingeless structures rotated using surface tension forces," *J. Microelectromech. Syst.*, vol. 4, pp. 177–184, Dec. 1995.

[5] I. Shimoyama, O. Kano, and H. Miura, "3D micro-structures folded by Lorentz force," in *Proc. 11th Annual International Workshop on Micro Electro Mechanical Systems*, Heidelberg, Germany, Jan. 25–29, 1998, pp. 24–28.

[6] Y. Li and C. Liu, "Assembly of micro optical components using magnetic actuation," in *The 10th Int. Conf. Solid-State Sensors and Actuators*, Sendai, Japan, Jun. 7–10, 1999, pp. 1466–1469.

[7] G. F. Weston, "Measurement of ultra-high vacuum. Part I. Total pressure measurements," *Vacuum*, vol. 29, no. 8/9, pp. 277–291, Aug.–Sept. 1979.

[8] K. F. Bohringer, K. Goldberg, M. Cohn, R. Howe, and A. Pisano, "Parallel microassembly with electrostatic force fields," in *Proc. IEEE Int. Conf. Robotics and Automation*, vol. 2, Leuven, Belgium, May 16–20, 1998, pp. 1204–1211.

[9] F. Dinelli, S. K. Biswas, G. A. D. Briggs, and O. V. Kolosov, "Ultrasound induced lubricity in microscopic contact," *Appl. Phys. Lett.*, vol. 71, no. 9, pp. 1177–1179, Sept. 1997.

[10] V. Kaajakari, S.-H. Kan, L.-J. Lin, A. Lal, and S. Rodgers, "Ultrasonic actuation for MEMS dormancy-related stiction reduction," in *Proceedings of the SPIE*, vol. 4180, Santa Clara, CA, Sept. 20, 2000, pp. 60–65.

[11] V. Kaajakari and A. Lal, "Pulsed ultrasonic release and assembly of micromachines," in *Proc. The 10th Int. Conf. Solid-State Sensors and Actuators*, Sendai, Japan, June 7–10, 1999, pp. 212–215.

[12] V. Kaajakari, S. Rodgers, and A. Lal, "Ultrasonically driven surface micromachined motor," in *Proc. 13th Annual Int. Workshop on Micro Electro Mechanical Systems*, Miyazaki, Japan, Jan. 23–27, 2000, pp. 40–45.

[13] J. H. de Boer, *The Dynamical Character of Adsorption*. New York: Oxford University Press, 1953.

[14] S. C. Saxena and R. K. Joshi, "Thermal accommodation and adsorption coefficients of gases," in *McGraw-Hill/CINDAS Data Series on Material Properties*. New York: McGraw Hill, 1981, vol. II-1.

[15] A. Roth, *Vacuum Technology*, 2nd ed. Amsterdam, The Netherlands: North-Holland, 1982.

[16] V. Kaajakari and A. Lal, "Electrostatic batch assembly of surface MEMS using ultrasonic triboelectricity," in *Proc. 14th Annual International Workshop on Micro Electro Mechanical Systems*, Interlaken, Switzerland, Jan. 21–25, 2001, pp. 10–13.

[17] H. L. Eschbach and R. Y. Werz, "A generalized correction factor for the Knudsen radiometer gauge with arbitrary vane and heater shape," *Vacuum*, vol. 26, no. 2, pp. 67–71, Feb. 1976.

[18] K. J. S. Pister, M. W. Judy, S. R. Burgett, and R. S. Fearing, "Automated assembly of flip-up micromirrors," *Sens. Actuators, Phys. A*, vol. A33, no. 3, pp. 249–256, June 1992.

Ville Kaajakari was born in Finland in 1975. He studied physics at the Helsinki University and electrical engineering in Helsinki University of Technology before continuing his studies in United States. He received the M.S. and Ph.D. degrees in electrical and computer engineering from University of Wisconsin-Madison in 2001 and 2002, respectively.

Since 2002, he has been a Postdoctoral Visiting Scientist at the VTT Information Technology, Finland, where his current research interest is in RF-MEMS.

Dr. Kaajakari was the winner of the IEEE International Ultrasonics Symposium student paper competition in 2001.

Amit Lal received the B.S. degree from California Institute of Technology, Pasadena, and the Ph.D. degree from University of California, Berkeley, in 1990 and 1996, respectively, both in electrical engineering. His Ph.D. work focused on high-intensity micromechanical ultrasonic actuators.

He is currently an Assistant Professor in the School of Electrical and Computer Engineering at Cornell University. From 1998 to 2002, he was an assistant professor at the University of Wisconsin-Madison. He currently leads the SonicMEMS laboratory focusing on ultrasonic and nonlinear ultrasonics applications for and of MEMS. His current focus is on the use of silicon-based high-intensity ultrasonic actuators with integrated sensors for microsurgical and microfluidic applications. His group also is also investigating the use of radioactive thin films in MEMS. He is the recipient of the NSF-CAREER award.